Geojournal of Tourism and Geosites
ISSN 2065-0817, E-ISSN 2065-1198

Year XIX, vol. 67, no. 3, 2026, p.2020-2033
DOI 10.30892/gtg.67317-1829

# INTEGRATED CA-MARKOV AND GEO-IT MODELING OF FUTURE LAND USE CHANGE IN SAMUI ISLAND, SURAT THANI PROVINCE, THAILAND

**Nanthaporn USAARD** [1], **Katawut WAIYASUSRI** [2*], **Dolreucha SUWANMAJO** [3], **Thipphaphone KEOVILIYAVONG** [4]

[1] Mahasarakham University, Faculty of Humanities and Social Sciences, Department of Geography, Mahasarakham, Thailand; nanthaporn.u@msu.ac.th (N.U.)
[2] Suan Sunandha Rajabhat University, Faculty of Humanities and Social Sciences, Geography and Geo-informatics Program, Bangkok, Thailand; katawut.wa@ssru.ac.th (K.W.)
[3] Alpha I Energy co., Ltd, Bangkok, Thailand; dolreucha.s@alphaiall.com (D.S.)
[4] National University of Laos, Faculty of Social Sciences, Department of Geography and Information Science, Vientiane, Laos; t.keoviliyavong@nuol.edu.la (T.K.)

**Citation:** Usaard, N., Waiyasusri, K., Suwanmajo, D., & Keoviliyavong, T. (2026). Integrated CA-Markov and Geo-IT modeling of future land use change in Samui Island, Surat Thani Province, Thailand. *Geojournal of Tourism and Geosites*, 67(3), 2020–2033. https://doi.org/10.30892/gtg.67317-1829

**Abstract:** Samui Island is a world-class marine tourism destination and a key economic driver for Thailand. Over the past several decades, Samui Island has experienced rapid spatial transformation. Development to support the tourism industry has led to rapid land use changes. The objective of this research is to analyze changes in land use patterns around Samui Island, Thailand, between 2006 and 2024 using Geo-information Technology (Geo-IT). Land use classification was performed from Landsat satellite images at each time period using the Random Forest classification method to detect and track changes in each type of land use. Future land use patterns in 2042 were then modelled using the CA-Markov model. Research results showed that in 2006, the majority of Samui Island's land area was covered by coconut, accounting for over 58.03% of the total area (137.28 km$^2$). This area is located on the steep slopes of the central part of Samui Island. After 18 years, the area under coconut cultivation decreased, and the area was transformed into durian plantations and villages. The overall accuracy of land use classification was 84.1%, 81.7%, and 75.3% in 2024, 2014, and 2006, respectively. A CA-Markov model simulation of land use patterns for the year 2042 shows that over the next 18 years, land use patterns for City, Town, Commercial (U1), and Institutional (U3) land use categories will increase by 1044.05% and 1050.27%, respectively. Urban expansion in the northeastern part of Samui Island, in the Bo Phut area, has seen grass land transformed into villages. In the southern part of Samui Island, around Na Mueang, Paddy Field has been transformed into a village, the same as the western part of Samui Island, around Taling Ngam. The results highlight the predicted spatial and temporal dynamics of land use changes in Samui Island, revealing land use changes resulting from urban expansion and agricultural expansion, particularly coconut and durian, which are local cash crops. Therefore, it is imperative to monitor the areas that are sensitive to the changes occurring in the plain landscape around the island, especially the areas of Paddy field, Grass land, Forest land, Orchards, and Perennial crops that are often converted into urban areas and villages. However, this research provides spatially-based land use data that will be useful for effective land use development planning in coastal tourism cities. This data will support decision-making in preparing for sustainable tourism development in the future.

**Keywords:** Future Land Use Change, CA-Markov Model, Geo-IT, Ko Samui Island, Surat Thani

* * * * * *

## INTRODUCTION

Land use changes (LUC) in islands has more complex and severe impacts than on mainland areas (Oktavia et al., 2024; Han et al., 2024). This is because islands have limited, fragile ecosystems and limited natural resources (Moustakas et al., 2025; Wayesa et al., 2025). Forest and agricultural areas are inevitably affected by urban expansion and construction (Mustelier & Henríquez, 2024; Thien et al., 2025). The main impacts of LUC on the island can be divided into three main areas: environmental and ecological, resource, and socio-economic. Environmental and ecological impacts, such as destruction of local animal and plant habitats, coastal degradation, natural disasters (flood, landslide etc.) (Dieno & Pathan, 2025; Tsumita et al., 2025; Aldiansyah et al., 2025).

The impacts of limited resources include freshwater shortages, soil erosion, and waste disposal problems on the island (Kamaraj & Rangarajan, 2022; Bikis et al., 2025). And, social and economic impacts include land use conflicts, local economic vulnerability, and changes to traditional cultures and ways of life (Quintas-Soriano et al., 2022).

[*] Corresponding author

Tourism is one of the most important drivers of land use change in areas with tourism potential, such as islands, coasts, or important World Heritage sites (Rimba et al., 2021; Liu et al., 2025; Ibarra-Núñez & Ortega-Rubio, 2025). This is often associated with the expansion of buildings, and the reduction of natural and agricultural areas (Birthal et al., 2021). Tourism acts as a magnet, attracting investment and creating demand for land in ways that are not conventional, leading to a rapid and intensive shift from traditional land use to commercial use. Research on the use of Geo-IT has often been applied to assess land use in major tourist cities such as Guangxi. It has been found that the majority of land use patterns are forested, but by 2020, the area will be affected by a shift from forestry to agriculture. It was also found that wetlands are decreasing (Qiu et al., 2021). In Hainan Island, the ecological system has been severely impacted by LUC for tourism development, with forest areas being converted into cities and farmland (Yang et al., 2024). Zhangjiajie, China, has been seen the largest increase in built-up area during 2000-2020, with most of its farmland and grasslands converted to built-up areas. The main cause is the shift to land use for tourism-related construction (Wang et al., 2023). In São Paulo, urban expansion has been found to have an impact on the area's freshwater resources, causing water shortages for the tourism sector (Petroni et al., 2022).

Tourism affects the physical processes of an area, particularly its natural resources and socio-economic aspects. For example, a study conducted in the tourist town of Menfi (Italy) found that during 2007-2022, there was a decrease in the area of grape cultivation, and an increase in the area for residential tourism (second homes). This, along with the cultivation of olives, has resulted in significant soil erosion. The main drivers are socioeconomics and the shift to olive cultivation in low-lying areas with landscape value (Tonolli et al., 2024). In the Sungai Karang coastal area (Malaysia), there was a rapid expansion of resorts and coastal infrastructure during 1966-2013 (Marzuki et al., 2024). Kolkata, India, during 2005-2019, experienced rapid urbanization, resulting in a decrease in vegetation cover, particularly in the urban core, and an increase in built-up area, which in turn increased surface temperatures (Chatterjee & Majumdar, 2022).

And in Ubud, Bali, they have analyzed the transformation of courtyard spaces to support sustainable tourism based on the principles of the Culture of Harmony. Qualitative research findings revealed that most courtyard areas (Palemahan or Teba), formerly used for animal breeding, raising/removing dirt, and gardening, have been transformed into tourist accommodations. Quantitative findings confirmed that this transformation has had positive economic, social, cultural, and environmental impacts, supporting sustainable tourism (Waridin & Astawa, 2021).

Therefore, it is imperative to urgently study LUC in major tourist destinations like Samui Island to prepare for economic growth while preserving quality of life, the environment, and local identity.

Samui Island is the second largest island in Thailand. It is located on the eastern coast of southern Thailand in the Gulf of Thailand. The word "Samui" has several uncertain origins, but the most reliable hypothesis is that it comes from the southern Tamil word "Samoi," meaning "waves," which later became corrupted into "Samui." Other theories suggest that the name comes from the Hainanese word "shao mui," which means "first checkpoint," or from the name of a tree called "mui," which grows widely on the island. Samui Island is a world-class marine tourism destination and a key economic driver for Thailand (Pongponrat, 2022; Iabsap & Phucharoen, 2025). Known for its beautiful beaches, crystal-clear waters, and iconic coconut groves, Samui Island has become a popular destination, attracting tourists from around the world. Over the past several decades, Samui Island has experienced dramatic spatial changes. Rapid development to support the tourism industry has led to the most pronounced changes in land use (Mustafa et al., 2019; Pongsakornrungsilp & Pongsakornrungsilp, 2023). The area has rapidly transformed from agricultural areas, particularly coconut plantations, into service areas. These areas have been intensively converted into hotels, resorts, vacation homes, and various tourism infrastructure. The expansion of construction has significantly diminished the original landscape of "Coconut Island" (Ubonsri & Daungthima, 2024). This shift, particularly in the easily accessible coastal plain, reflects a complete economic shift from agriculture to the service sector. Spatial changes on Samui Island thus fully transform from an agricultural society into an international tourism hub. This has resulted in challenges in natural resource management, environmental impacts, and social pressures from rising land prices and the cost of living in the area. Therefore, sustainable management requires robust spatial planning to control urban expansion and strike an appropriate balance between economic growth and the sustainable preservation of the island's natural and cultural identity.

The objective of this research is to analyze land use pattern changes on Samui Island, Thailand, between 2006 and 2024 using geoinformatics technology and to model future land use patterns through 2042 using a CA-Markov model. This research utilized land use classification from Landsat satellite imagery at different times to detect and track changes in different land use types. This research process aligns with the Sustainable Development Goals (SDGs). Especially SDG 11, Sustainable Cities and Communities, as it contributes to understanding urban sprawl caused by tourism (Kelly-Fair et al., 2022; Enoh et al., 2023; Estoque et al., 2021; Ferdos et al., 2026). This research aims to inform urban planning and determine effective land use control measures. This research helps predict and prevent the loss of important areas, such as forests or agricultural areas. This aligns with SDG 15: Life on land, protecting and restoring terrestrial ecosystems (Cao et al., 2023; Utama et al., 2024). It also supports SDG 8: Decent work and economic growth by promoting sustainable tourism that balances economic benefits with the preservation of natural resources and the environment, which are the heart of long-term tourism (Song et al., 2023; Appelt et al., 2022; Suhud et al., 2025). The expected outcomes of this research include empirical spatial data and tools for policy decision-making. In particular, historical land use change maps and models predicting future urban expansion patterns will be obtained. This will enable local authorities to more effectively plan urban planning and implement land use control measures, preventing encroachment on environmentally sensitive areas and planning appropriate infrastructure and utility investments. Furthermore, these results provide an important foundation for promoting sustainable tourism by balancing economic growth with the long-term conservation of Samui Island's natural resources and unique identity.

## MATERIALS AND METHODS

### Study area and Background

Samui Island is the largest island in the Gulf of Thailand and the second largest after Phuket (Iabsap & Phucharoen, 2025). It covers an area of 236.57 $km^2$. Samui Island is located between latitudes 9°20' N to 9°40' N and longitudes 99°50' N to 100°10' N (Figure 1). Samui Island is located northeast of Surat Thani Province in the Gulf of Thailand, approximately 84 km off the coast. Samui Island's main topography is a mountainous region in the central part of the island, straddling the northwest to southeast. The highest peak is Khao Pom, at 645 m. high. The surrounding area is a coastal plain, which is why most settlements are located on this terrain (Bai et al., 2021).

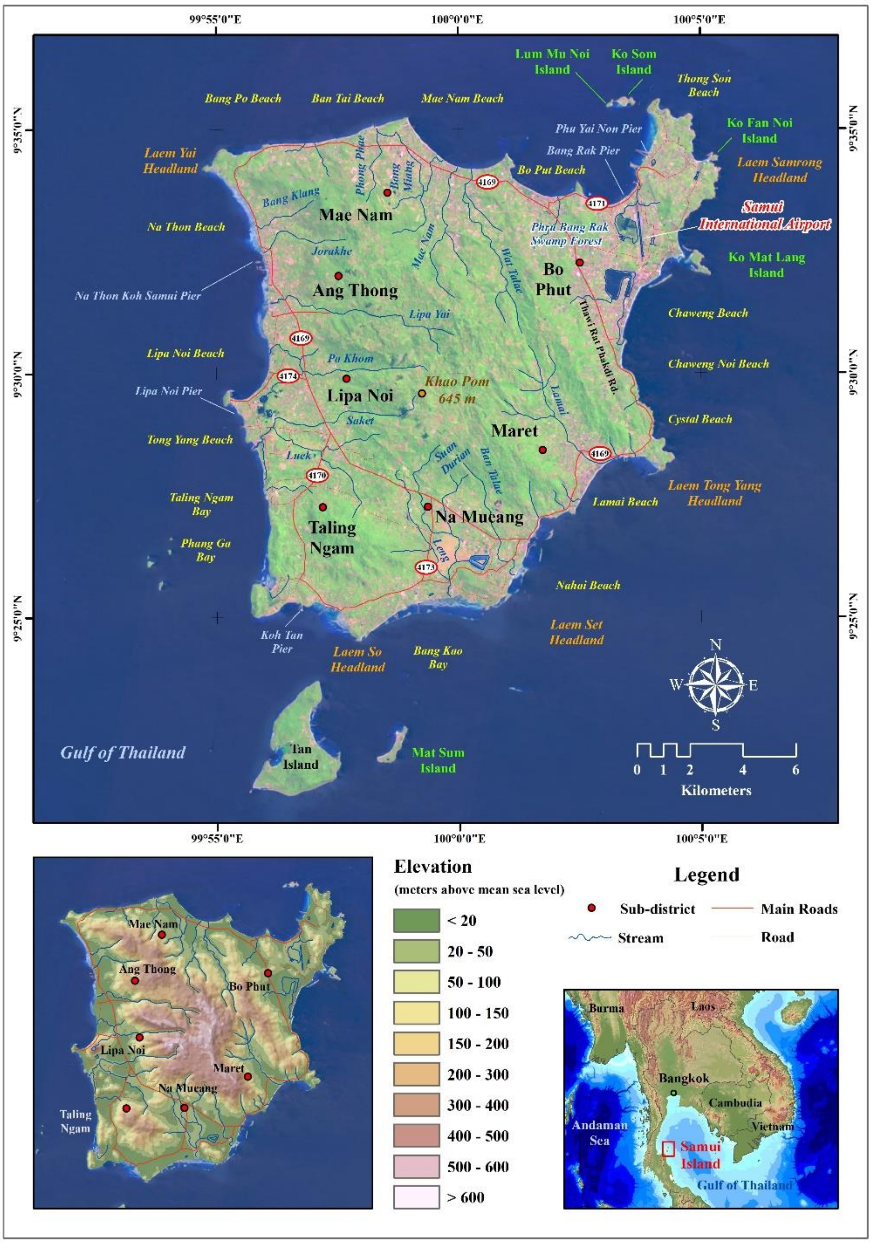


Figure 1. Location of Samui Island, Surat Thani Province, Thailand (Source: Collected and processed by authors)

The largest coastal plain covers the northeastern part of Samui Island, where Bo Phut subdistrict is located. This area has beautiful coastline and beaches, including Chaweng and Chaweng Noi beaches, which are the most beautiful on Samui Island. It is also home to Samui International Airport. The southern part of the island features a narrow coastal plain with beautiful beaches like Lamai and Nahai, located between Laem Tong Yai and Laem Set headlands. The southern part of the island features indented bays, including Bang Kao, Phang Ga, and Taling Ngam bays. The western part of the island features a long coastal plain with important beaches like Tong Yang, Lipa Noi, and Na Thon. Na Thon Beach is home to a major transport pier, Na Thon Koh Samui Pier, for travel between the island and the mainland.

The northern part of the island, from Laem Yai Headland to Laem Samrong Headland, features a long coastal landscape that extends to the northeastern coastal plain. Important beaches include Bang Po, Ban Tai, Mae Nam, Bo Put, and Thong Son beaches (Yeemin et al., 2024). Laem Samrong Headland is also home to important ports for travel between other major islands in the Gulf of Thailand, namely Bang Rak and Phu Yai Non Pier. Samui Island's drainage system is characterized by a radial drainage system. Controlled by geological features, the central part of the island is a large Triassic igneous rock mountain range (Nazaruddin, 2020). As the mountain range was eroded by rainwater and streams, it formed a coastal plain around Samui Island, covered with modern sedimentary rocks, known as Quaternary Alluvial Deposits. The major drainage systems are: 1) River systems flowing into the Gulf of Thailand to the north, including the Phong Phae, Bang Miang, Mae Nam, and Wat Talea streams. 2) River systems flowing into the Gulf of Thailand to the south, including the Lamai, Ban Talae, Suan Durain, and Leng streams. And, 3) River systems flowing into the Gulf of Thailand to the east, including the Bang Klang, Jorakhe, Lipa Yai, Pa Khom, Saket, and Luek streams.

Tourism on Samui Island began in the 1970s with backpackers seeking the pristine nature, tranquil beaches, and simple island lifestyle. At that time, the main occupation of Samui Island residents was coconut farming, which led to the image of the "Coconut Island" alongside the beauty of the sea. In the 1980s, tourism on Samui Island began to expand rapidly, driven by infrastructure development. A pier and a road around the island, Thawi Rat Phakdi Road (Highway 4169), were built, making travel easier. In 1989, Bangkok Airways Public Company Limited opened Samui Airport, making travel from Bangkok convenient and faster, attracting more premium tourists (Vu & Turner, 2006).

Furthermore, investment in numerous world-class hotels and resorts has enabled Samui Island to cater to a diverse range of tourist groups, from backpackers to high-end travelers. Samui Island also boasts tourism resources, particularly its natural beauty, such as its beautiful beaches, such as Chaweng, Lamai, and Bophut. This has resulted in a variety of tourism activities, including water activities (snorkeling, scuba diving, kayaking, jet skiing, etc.), cultural activities such as temples and local communities, nature and adventure tourism such as trekking to waterfalls, an open zoo, ATV rides, and health tourism such as massage and spas, which are abundant on Samui Island.

**Data Preparation**

This research collected satellite imagery from Landsat 5TM, 8OLI/TIRS, and 9 OLI/TIRS satellites, covering the years 2006, 2014, and 2024, respectively (Table 1). These satellite images are available from the U.S. Geological Survey. Band combinations were then performed in ArcMap 10.8 software to obtain easily interpretable land cover and various land use patterns to track land use change over time. Band combinations were performed this time. Landsat 5TM satellite imagery has been blended with the R: G: B band of 543, which is a combination of short-wave infrared, near-infrared, and red bands (Thien et al., 2025; Le et al., 2025). Landsat 8OLI/TIRS and Landsat 9OLI/TIRS satellite imagery have been blended with the R: G: B band of 654, which is a combination of short-wave infrared, near-infrared, and red bands (Sales et al., 2023). Once the satellite imagery from the three time periods was acquired, it was processed through the Satellite Imagery Cloud Removal and Correction process, as satellite imagery covering the study area often exhibits cloud cover almost year-round due to the tropical equatorial climate. Radiometric correction using standard deviation was then performed to obtain sharper satellite imagery prior to land cover interpretation (Du et al., 2002; Hantson & Chuvieco, 2011).

Table 1. Satellite Image data over the Ao Nang area, Krabi Province

| Database | Red:Green: Blue (R:G:B) | Path/Row | Resolution | Acquisition date | Format | Sources |
|---|---|---|---|---|---|---|
| Landsat 5TM | 5:4:3 | 129/53 | 30 m | 1 April 2006 | Image file | https://earthexplorer.usgs.gov/ |
| Landsat 8 OLI/TIRS | 6:5:4 | 129/53 | 30 m | 13 June 2014 | Image file | https://earthexplorer.usgs.gov/ |
| Landsat 9 OLI/TIRS | 6:5:4 | 129/53 | 30 m | 13 August 2024 | Image file | https://earthexplorer.usgs.gov/ |

**METHODOLOGY**

The research process includes the Geo-IT process and the CA-Markov model, as shown in Figure 2. Details of each step are briefly explained below:

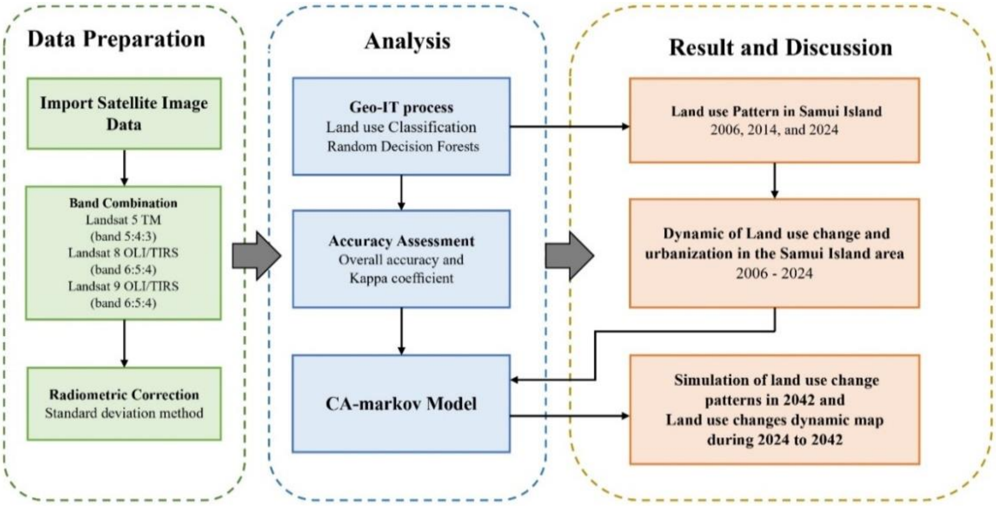


Figure 2. Flow chart of methodology

**Geo-IT process**

Geo-IT is a process that combines remote sensing and GIS. This research applied Geo-IT to land use and land cover classification. In this step, satellite imagery from three time periods (2006, 2014, and 2024) was imported into ArcGIS 10.8 software to analyze land use classification using machine learning principles. This approach utilises deep learning classification techniques, such as Random Decision Forests (or Random Forest), an ensemble learning method for land use and land cover classification. The Random Decision Forests method is a popular method for efficiently interpreting land use (Phinzi et al., 2023). Random Forest is a classification method that relies on an ensemble of decision trees. By combining the predictions of multiple weak learners, it generally attains higher accuracy than any single tree. The model's final output is produced by aggregating the decisions of all trees in the ensemble, most often through majority voting (Rodriguez-Galiano et al., 2012; Avci et al., 2023). The training process for a Random Forest is incremental, with decision trees added sequentially. After each tree is built, the algorithm assesses the model's performance using out-of-bag (OOB) samples. These samples are run through the forest, and their predicted labels are determined via majority voting (Jamali et al., 2024). The importance or contribution of each feature to an individual tree is then computed as described in Equation 1 (Krishna & Gopinath, 2022).

$$fi_i = \frac{\sum_{j:node\ j\ splits\ on\ feature\ i} ni_j}{\sum_{k\in all\ nodes} ni_j} \qquad (1)$$

Where $fi_i$ is the importance of feature $i; ni_j$ is the importance of node j. These can then be normalized to a value between 0 and 1 by dividing by the sum of all feature importance values (Equation 2) (Krishna & Gopinath, 2022):

$$normfi_i = \frac{fi_i}{\sum_{j\in all\ features} fi_i} \qquad (2)$$

The final feature importance, at the Random Forest level, is its average over all the trees. The sum of the feature's importance value on each tree is calculated and divided by the total number of trees (Equation 3) (Krishna & Gopinath, 2022):

$$RFfi_i = \frac{\sum_{j\in all\ trees} normfi_{ij}}{T} \qquad (3)$$

Where $RFfi_i$ is the importance of feature i calculated from all trees in the Random Forest model; $normfi_{ij}$ is the normalized feature importance for i in tree j; and $T$ is total number of trees. The results of the land use pattern interpretation are displayed as the overall accuracy and Kappa coefficient (KHAT) to assess the accuracy of the classification of various data that appear on satellite imagery (Foody, 2020; Chaaban et al., 2022). Sampling points in the study area were determined based on data from the Land Development Department (LDD), Thailand. To evaluate classification accuracy, this study utilizes the confusion matrix, overall accuracy (OA), and kappa coefficient. The matrix distinguishes between correct assignments (diagonal) and misclassifications (off-diagonal), specifically identifying commission errors (FP) that impact precision and omission errors (FN) that represent missed targets. Overall accuracy is derived from the ratio of correct predictions (TP + TN) to total samples. Additionally, the kappa coefficient accounts for chance-based agreement; values near +1 reflect high model reliability, whereas negative values suggest systematic discrepancies between classified results and reference data. The OA was calculated based on Equation 4 and the kappa coefficient calculated using Equation 5 (Sarvestani et al., 2025):

$$Overall\ accuracy\ = \frac{TP+TN}{TP+FP+TN+FN} \qquad (4)$$

where *TP* is the number of correct positive predictions, *TN* is the number of correct negative predictions, *FP* is the commission error, and *FN* is the omission error.

$$\text{Kappa coefficient} = \frac{p_0-p_e}{1-p_e} \qquad (5)$$

where $P_0$ is the observed accuracy, and $P_e$ is the expected accuracy.

The validation was performed compared with the data obtained from the classification. The classification criteria were as follows (Herano et al., 2025): < 0 means unacceptable classification data; 0.01 – 0.40 means fair classification data; 0.41 – 0.60 means moderate classification data; 0.61 – 0.80 means good classification data; 0.81 – 1.00 means very good classification data. After validation of the data obtained from the land use pattern interpretation, the data that passed the Overall Accuracy and KHAT criteria were analyzed for land use change using the Change Detection method in the Tabulate area analysis function in ArcGIS 10.8 software. The change detection analysis can be calculated as Equation 6 (Puyravaud, 2003; Kiriwongwattana & Waiyasusri, 2024):

$$\Delta = [(A_2 - A_1) / A_1 \times 100] / (T_2 - T_1) \qquad (6)$$

Where Δ is the percentage change in land use pattern. $A_1$ is the land use type at time one ($T_1$). $A_2$ is the land use type at time two ($T_2$). The results are displayed as the land use proportions of each type on a transition matrix map, which shows the land use change patterns from 2006 to 2024 on Samui Island.

**CA-Markov model**

The CA–Markov model is a dynamic, multi-scale, spatially explicit, raster-based approach capable of identifying locations with a high likelihood of future land use change (Guan et al., 2011; Jafari et al., 2016; Xu et al., 2023). In this framework, the CA–Markov component functions as the non-spatial demand module, estimating land use transitions over a series of years at an aggregate level. Markov chain analysis, a stochastic method, characterizes how specific conditions evolve step by step within a land use geospatial dataset. The model is built using land use distributions at the start ($X_t$) and end ($X_{t+1}$) of a discrete time interval, along with a transition matrix ($X_{LU}$) that captures the LUC occurring during that period. The values in this matrix come directly from classifying the three multispectral Landsat images using the maximum likelihood algorithm, expressed as the proportion of each land use category (Adhikari & Southworth, 2012). This matrix is then used to establish the "link'' in the Markov chain, as represented in Equation 7.

$$P_{i,j} \times i_t = i_{t+1}, \qquad \begin{bmatrix} P_{uu} & P_{ua} & P_{uw} \\ P_{au} & P_{aa} & P_{aw} \\ P_{wu} & P_{wa} & P_{ww} \end{bmatrix} \begin{bmatrix} U_t \\ A_t \\ W_t \end{bmatrix} = \begin{bmatrix} U_{t+1} \\ A_{t+1} \\ W_{t+1} \end{bmatrix} \tag{7}$$

where $t$ is the time (Year), $P_{i,j}$ is the transition probability matrix of the land use class $i$ change to class $j$. $i$ and $j$ are the land use classes in the first year and the second year, respectively. The CA-Markov analysis was used to determine the demand for the probability of each land use pattern, where the probability of transition ($P_{i,j}$) is given for every ordered set of conditions. In a CA-Markov with a limited number of conditions, such as $j$, a new transition probability matrix is bounded, as in Equation 8 (Butt et al., 2015):

$$V_j \times P_{jk} = [V_1, V_2, V_3, \dots, V_n] \begin{bmatrix} P_{11} & P_{12} & \dots & P_{1m} \\ P_{21} & P_{22} & \dots & P_{2m} \\ P_{31} & P_{32} & \dots & P_{3m} \\ \vdots & \vdots & & \vdots \\ P_{n1} & P_{n2} & \dots & P_{nm} \end{bmatrix}, \tag{8}$$

Where $Vj \times Pjk$ is the proportion of land use in the second year; $P_{jk}$ is the land use activity (f) derived from the transition probability matrix; $V_j$ is the proportion of land use in the first year; $j$ is the type of land use in first year and; $k$ is the type of land use in the second year. The results of the model will provide spatially representative land use data for 2042. This data will be used to plan island development and prepare for future spatial changes in the Samui Island area.

## RESULTS

### Land use pattern in Samui island area

Classifying land use patterns from Landsat satellite imagery from three time periods: 2006, 2014, and 2024, using the Random forest classification method, resulted in this research on the land use patterns in Samui. There are 15 types of island classifications: Paddy field (A1), Perennial crops (A3), Perennial crops (A4), Durian (A403), Coconut (A405), Forest land (F), Grass land (M1), Mineral (M3), Beach (M6), City, Town, Commercial (U1), Villages (U2), Institutional land (U3), Transportation (U4), Recreation area (U6), and Water bodies (W). The overall accuracy assessment of land use classification was 84.1%, 81.7%, and 75.3% in 2024, 2014, and 2006, respectively, with a Kappa coefficient of 0.81, 0.78, and 0.70, respectively. The classification results are considered good to very good.

In 2006, the majority of Samui Island's land use, over 58.03% of the total area (137.28 km²), was used for coconut cultivation. This is because the study area has long been a coconut-growing region, a local economic crop and a fundamental part of the Samui islanders' way of life, earning it the nickname "Coconut Island." The most popular coconut variety is the Samui Cooking Coconut. This variety has been renowned and cultivated for over 100 years due to its large size, good weight, rich and delicious coconut milk, and its acceptance in the market. The second most common land use on Samui Island was Forest land (16.33% of the total area), and Villages (8.60% of the total area), respectively. The second most popular crop after coconut was durian, covering 5.66% of the total area (13.38 km²). The majority of durian plantations are located in the central part of Samui Island. This area is characterized by mountainous and sloping terrain on the island. The most popular durian varieties grown are Monthong, Chanee, and Met Nai Samui. Monthong is the most popular variety for commercial cultivation and export to China. Chanee is primarily grown commercially domestically. Met Nai Samui is a rare local variety currently being developed and propagated on Samui Island.

Table 2. Land use pattern statistics in Samui island area in 2006, 2014, and 2024 ($km^2$) (Source: Processed by authors)

| Land Use Pattern | | 2006 | | 2014 | | 2024 | | Area Change ($km^2$) | | |
|---|---|---|---|---|---|---|---|---|---|---|
| | | $km^2$ | % | $km^2$ | % | $km^2$ | % | 2006 to 2014 | 2014 to 2024 | 2006 to 2024 |
| A1 | Paddy field | 6.83 | 2.89 | 6.71 | 2.84 | 5.86 | 2.48 | -0.12 | -0.85 | -0.97 |
| A3 | Perennial crops | 8.48 | 3.58 | 6.20 | 2.62 | 5.96 | 2.52 | -2.28 | -0.24 | -2.52 |
| A4 | Orchards | 1.68 | 0.71 | 12.79 | 5.41 | 9.74 | 4.12 | 11.11 | -3.05 | 8.06 |
| A403 | Durian | 13.38 | 5.66 | 19.04 | 8.05 | 20 | 8.45 | 5.66 | 0.96 | 6.62 |
| A405 | Coconut | 137.28 | 58.03 | 68.81 | 29.09 | 61.19 | 25.86 | -68.47 | -7.62 | -76.09 |
| F | Forest land | 38.63 | 16.33 | 58.95 | 24.92 | 57.29 | 24.22 | 20.32 | -1.66 | 18.66 |
| M1 | Grass land | 1.51 | 0.64 | 15.26 | 6.45 | 24.99 | 10.56 | 13.75 | 9.73 | 23.48 |
| M3 | Mineral | 0.22 | 0.09 | 0.55 | 0.23 | 1.30 | 0.55 | 0.33 | 0.75 | 1.08 |
| M6 | Beach | 1.37 | 0.58 | 1.39 | 0.59 | 1.37 | 0.58 | 0.02 | -0.02 | 0.00 |
| U1 | City, Town, Commercial | 1.26 | 0.53 | 1.25 | 0.53 | 1.26 | 0.53 | -0.01 | 0.01 | 0.00 |
| U2 | Villages | 20.34 | 8.60 | 35.06 | 14.82 | 38.15 | 16.13 | 14.72 | 3.09 | 17.81 |
| U3 | Institutional land | 0.18 | 0.08 | 0.77 | 0.33 | 0.93 | 0.39 | 0.59 | 0.16 | 0.75 |
| U4 | Transportation | 1.42 | 0.60 | 1.67 | 0.71 | 1.76 | 0.74 | 0.25 | 0.09 | 0.34 |
| U6 | Recreation area | 2.25 | 0.95 | 4.40 | 1.86 | 4.58 | 1.94 | 2.15 | 0.18 | 2.33 |
| W | Water bodies | 1.75 | 0.74 | 3.73 | 1.58 | 2.2 | 0.93 | 1.98 | -1.53 | 0.45 |
| Total | | 236.58 | 100.00 | 236.58 | 100.00 | 236.58 | 100.00 | | | |
| Overall Accuracy (%) | | 75.30 | | 81.70 | | 84.10 | | | | |
| Kappa Coefficient | | 0.70 | | 0.78 | | 0.81 | | | | |

**Dynamic of land use change in the Samui island area during 2006 to 2024**

This research found that over the past 18 years, the area planted with coconut trees has decreased by more than 76.09 km², a reduction of over half. This change in coconut plantation area is due to the expansion of the tourism business and changes in the lifestyle of local people, shifting from agriculture to the tourism service sector. In addition, some coconut plantations have been replaced by other agricultural forms and expanded village areas. The trend shows that land use for durian, grass land, and villages is increasing exponentially. For example, durian cultivation has become the largest agricultural crop on Samui Island, surpassing coconuts in terms of production value. Turf land is awaiting conversion from traditional agriculture like coconut cultivation to construction or in preparation for expanding durian cultivation. Land use with less change includes paddy field, minerals, beach, city town and commercial, institutional land, and transportation. The proportions of each land use type are detailed in Figure 3 and Table 2.

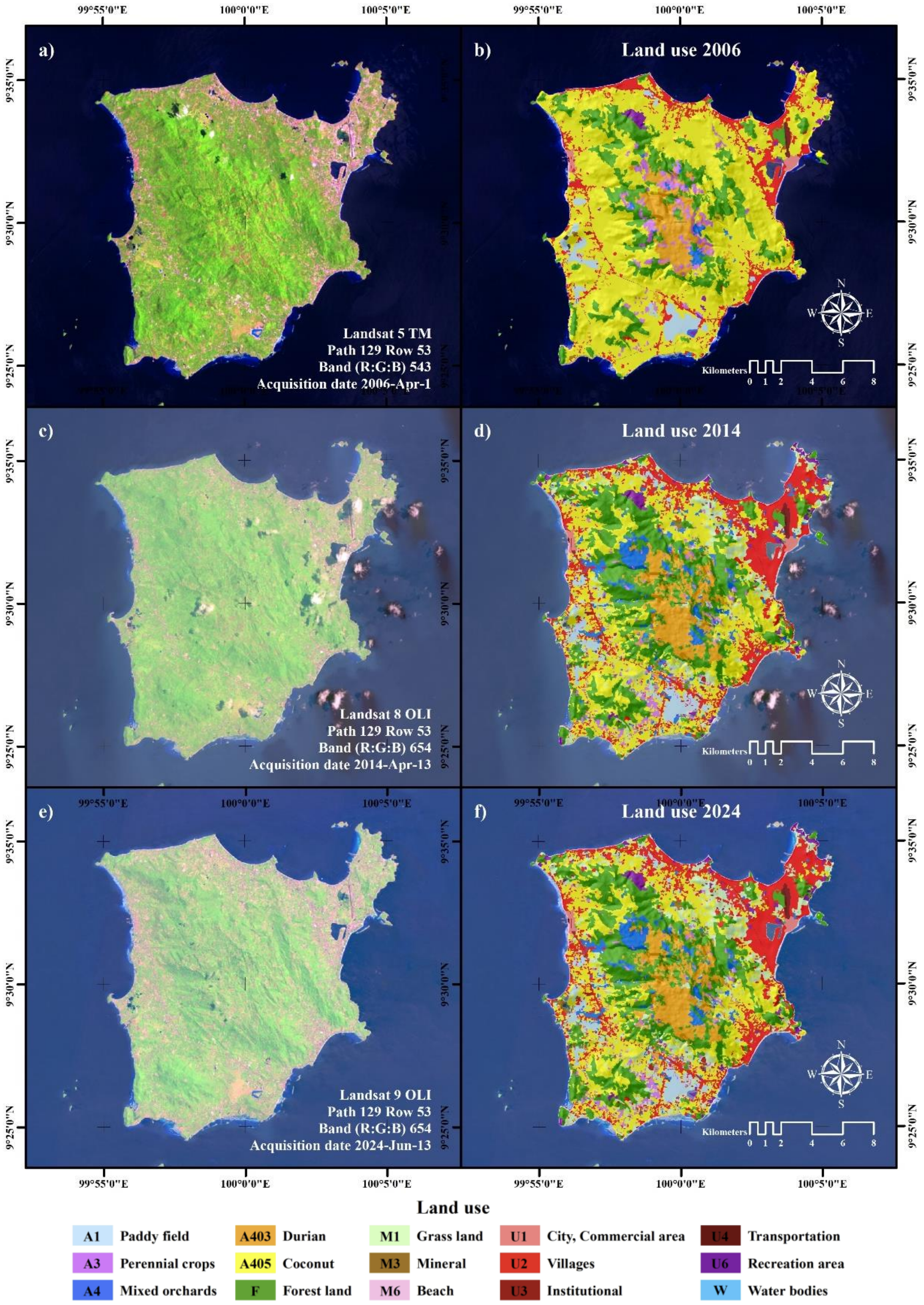


Figure 3. Landsat satellite imagery and land use pattern of Samui island area in 2006, 2014, and 2024 (Source: Collected and processed by authors)

Over the past 18 years, Samui Island has shown spatial changes, including changes in agricultural areas such as coconut, durian, and perennial plantations, as well as an increase in forest areas and urban expansion. Changes in land use between 2006 and 2024 were researched using the tabulate area method in ArcMap. The results are presented in the form of a metric table of LUC as shown in Table 3. This research found that, between 2006 and 2024, the most significant change in land use was observed in Samui Island, with a substantial increase of 1555.13% over the past 18 years. This type of land use, which was originally only 1.51 km², has now increased to 24.99 km².

Table 3. Matrix of Land use change in Samui island area during 2006 to 2024 ($km^2$)

| Land use change | | 2024 | | | | | | | | | | | | | | | | Changing Area | |
|---|---|---|---|---|---|---|---|---|---|---|---|---|---|---|---|---|---|---|---|
| | | A1 | A3 | A4 | A403 | A405 | F | M1 | M3 | M6 | U1 | U2 | U3 | U4 | U6 | W | Total | $km^2$ | % |
| 2006 | A1 | 4.87 | 0.13 | 0.10 | 0.02 | 0.13 | 0.03 | 0.53 | 0.22 | 0.00 | 0.00 | 0.50 | 0.12 | 0.00 | 0.02 | 0.16 | 6.83 | -0.97 | -14.21 |
| | A3 | 0.00 | 0.43 | 1.11 | 2.98 | 0.26 | 2.95 | 0.63 | 0.07 | 0.00 | 0.00 | 0.05 | 0.01 | 0.00 | 0.00 | 0.01 | 8.48 | -2.53 | -29.87 |
| | A4 | 0.00 | 0.02 | 1.26 | 0.04 | 0.06 | 0.25 | 0.03 | 0.00 | 0.00 | 0.00 | 0.01 | 0.00 | 0.00 | 0.00 | 0.02 | 1.68 | 8.06 | 479.46 |
| | A403 | 0.00 | 0.18 | 0.28 | 10.41 | 0.14 | 2.01 | 0.27 | 0.00 | 0.00 | 0.00 | 0.08 | 0.01 | 0.00 | 0.00 | 0.00 | 13.38 | 6.62 | 49.51 |
| | A405 | 0.82 | 4.70 | 5.55 | 4.22 | 57.34 | 20.99 | 20.36 | 0.83 | 0.03 | 0.05 | 19.51 | 0.23 | 0.21 | 2.13 | 0.32 | 137.28 | -76.09 | -55.43 |
| | F | 0.00 | 0.46 | 1.24 | 2.33 | 2.31 | 30.69 | 0.75 | 0.10 | 0.00 | 0.00 | 0.39 | 0.04 | 0.11 | 0.21 | 0.01 | 38.63 | 18.65 | 48.28 |
| | M1 | 0.00 | 0.00 | 0.00 | 0.00 | 0.00 | 0.00 | 1.51 | 0.00 | 0.00 | 0.00 | 0.00 | 0.00 | 0.00 | 0.00 | 0.00 | 1.51 | 23.48 | 1555.13 |
| | M3 | 0.00 | 0.00 | 0.00 | 0.00 | 0.00 | 0.00 | 0.18 | 0.02 | 0.00 | 0.00 | 0.01 | 0.00 | 0.02 | 0.00 | 0.00 | 0.23 | 1.08 | 477.78 |
| | M6 | 0.00 | 0.00 | 0.00 | 0.00 | 0.02 | 0.00 | 0.01 | 0.00 | 1.21 | 0.00 | 0.05 | 0.00 | 0.00 | 0.01 | 0.06 | 1.35 | 0.03 | 2.04 |
| | U1 | 0.00 | 0.00 | 0.02 | 0.00 | 0.00 | 0.01 | 0.00 | 0.00 | 0.00 | 1.16 | 0.02 | 0.02 | 0.04 | 0.00 | 0.00 | 1.27 | -0.02 | -1.38 |
| | U2 | 0.17 | 0.03 | 0.16 | 0.01 | 0.88 | 0.33 | 0.53 | 0.07 | 0.03 | 0.03 | 17.10 | 0.17 | 0.27 | 0.53 | 0.05 | 20.34 | 17.82 | 87.61 |
| | U3 | 0.00 | 0.00 | 0.00 | 0.00 | 0.00 | 0.01 | 0.01 | 0.00 | 0.00 | 0.00 | 0.03 | 0.14 | 0.00 | 0.00 | 0.00 | 0.18 | 0.75 | 422.54 |
| | U4 | 0.00 | 0.01 | 0.00 | 0.00 | 0.04 | 0.02 | 0.05 | 0.00 | 0.00 | 0.01 | 0.22 | 0.01 | 1.09 | 0.01 | 0.00 | 1.46 | 0.30 | 20.17 |
| | U6 | 0.00 | 0.00 | 0.01 | 0.00 | 0.01 | 0.00 | 0.17 | 0.00 | 0.02 | 0.00 | 0.14 | 0.19 | 0.02 | 1.67 | 0.02 | 2.24 | 2.34 | 104.58 |
| | W | 0.00 | 0.00 | 0.00 | 0.00 | 0.01 | 0.00 | 0.00 | 0.00 | 0.08 | 0.00 | 0.06 | 0.00 | 0.00 | 0.00 | 1.55 | 1.70 | 0.50 | 29.07 |
| | Total | 5.86 | 5.95 | 9.74 | 20.00 | 61.19 | 57.29 | 24.99 | 1.30 | 1.37 | 1.26 | 38.15 | 0.93 | 1.76 | 4.58 | 2.20 | | | |

This area is being prepared for future land use changes, such as durian cultivation, perennial tree plantations, or building construction. The second most significant change was in Orchards (A4), with a rate of change as high as 479.46%. Between 2006 and 2024, the proportion of this land use increased from 1.68 km² to 9.74 km². This is attributed to the increasing commercial cultivation of other fruit trees such as rambutan, mangosteen, and other fruits.

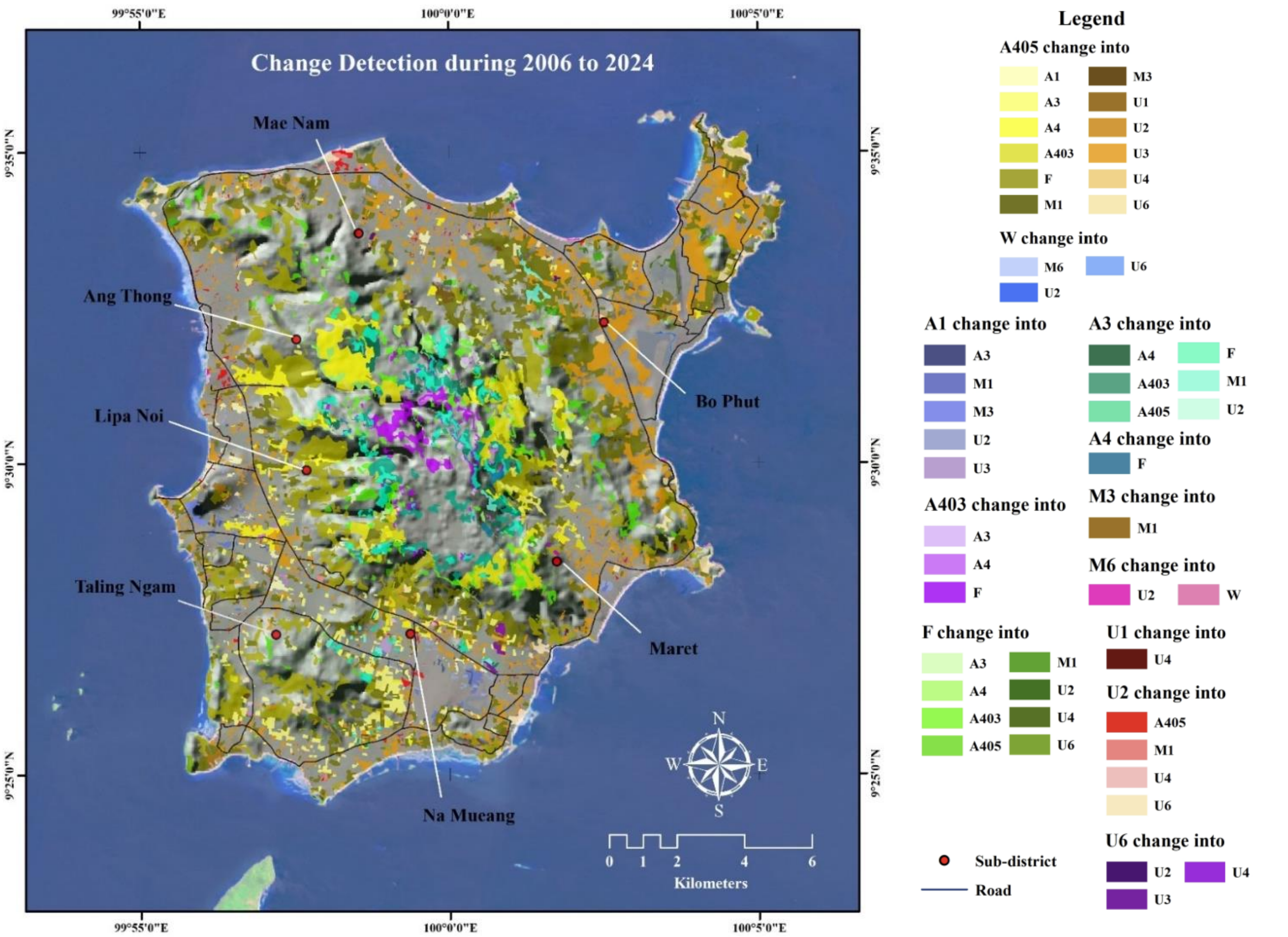


Figure 4. LUC dynamic map during 2006 to 2024 in Samui island area, Surat Thani Province (Source: Collected and processed by authors)

However, if we compare areas with the most significant land use changes, it would undoubtedly be coconut plantations. During 2006 to 2024, this area showed the largest decrease in land area, due to a land area reduction of 76.09 km$^2$. The coconut plantation area has been transformed into Forest land, Grass land, Villages, Orchards, Perennial crops, Durian, Recreation area, Minerals, Paddy field, Water bodies, Institutional land, Transportation, City Town Commercial, and Beach, respectively. The proportion of land changed to each of these land use types is 20.99, 20.36, 19.51, 5.55, 4.70, 4.22, 2.13, 0.83, 0.82, 0.32, 0.23, 0.21, 0.05, and 0.03 km$^2$, respectively.

Figure 4 shows the area changes in each land use type. It can be seen that the areas surrounding the sloping mountain range, where the coconut plantation was located, have been primarily transformed into forest land and durian orchards. In most lowlands, coconut plantations have been converted to fruit trees, perennial plants, and villages. Specifically in the southwestern plains of the island, most coconut plantations have been repurposed into fruit trees and perennial plants. The coastal area in the northeast (Laem Samrong) is also affected. In the northern and eastern parts of the island (along the Thawi Rat Phakdi Road (HW 4169)), most coconut plantations have been converted into villages. Coconut cultivation on Samui Island has declined significantly due to economic and land use changes. The expansion of tourism and real estate has led to the conversion of many coconut plantations into resorts and hotels. At the same time, unprofitable coconut prices and reduced competitiveness compared to other production areas have significantly hampered farmers' incentive to continue cultivation. Furthermore, pest infestations such as the black-headed caterpillar and black spiny beetle. In addition, the impact of erratic weather patterns further exacerbates the decline in yields, leading to a gradual decrease in the area planted with coconut trees, which are a symbol of the island.

**Simulation of land use change patterns with the CA-markov model in the Samui Island area**

The land use pattern simulation using the CA-Markov model shows the results of this research as follows: Over the next 18 years, land use patterns of City, Town, Commercial (U1) and Institutional land (U3) will increase by 1044.05% and 1050.27%, respectively. However, when compared in terms of area, land use patterns of Villages (U2) and City, Town, Commercial (U1) will see increases of 16.43 km$^2$ and 13.16 km$^2$, respectively. Table 4 shows the changes in land use patterns, indicating that Grass land (M1), Paddy field (A1), Durian (A405), Recreation area (U6), Forest land (F), Water bodies (W), Beach (M6), Orchards (A4), Perennial crops (A3), Mineral (M3), Institutional (U3), and City, Town, Commercial (U1) will see changes of 4.60, 4.41, and 13.16 km$^2$ respectively, respectively, as the land is transformed into Villages (U2). 3.22, 1.13, 1.11, 0.66, 0.50, 0.39, 0.37, 0.24, 0.17, and 0.04 km$^2$, respectively. Figure 4 shows areas with land-use change. In the northeast of Samui Island, in the Bo Phut area, grassland has been transformed into a village. Similarly, in the southern part of Samui Island, in the Na Mueang area, paddy fields have been transformed into villages. The same applies to the western part of Samui Island, in the Taling Ngam area.

Table 4. Matrix of Land use change in Samui Island area during 2024 to 2042 (km$^2$)

| Land use change | | 2042 | | | | | | | | | | | | | | | | Changing Area | |
|---|---|---|---|---|---|---|---|---|---|---|---|---|---|---|---|---|---|---|---|
| | | A1 | A3 | A4 | A403 | A405 | F | M1 | M3 | M6 | U1 | U2 | U3 | U4 | U6 | W | Total | km$^2$ | % |
| 2024 | A1 | 0.15 | 0.00 | 0.03 | 0.00 | 0.32 | 0.01 | 0.20 | 0.03 | 0.00 | 0.71 | 4.41 | 0.01 | 0.01 | 0.00 | 0.00 | 5.86 | -5.67 | -96.76 |
| | A3 | 0.01 | 0.22 | 0.04 | 0.20 | 4.47 | 0.40 | 0.17 | 0.00 | 0.00 | 0.07 | 0.37 | 0.00 | 0.00 | 0.00 | 0.00 | 5.95 | -1.69 | -28.37 |
| | A4 | 0.00 | 0.38 | 4.99 | 0.14 | 2.88 | 0.82 | 0.07 | 0.00 | 0.00 | 0.05 | 0.39 | 0.00 | 0.01 | 0.00 | 0.01 | 9.73 | -4.29 | -44.10 |
| | A403 | 0.00 | 1.15 | 0.09 | 15.78 | 1.95 | 0.96 | 0.08 | 0.00 | 0.00 | 0.00 | 0.00 | 0.00 | 0.00 | 0.00 | 0.00 | 20.00 | -2.79 | -13.95 |
| | A405 | 0.02 | 0.95 | 0.07 | 0.04 | 53.86 | 0.69 | 0.63 | 0.01 | 0.05 | 1.45 | 3.22 | 0.03 | 0.07 | 0.08 | 0.02 | 61.19 | 11.58 | 18.92 |
| | F | 0.00 | 1.43 | 0.15 | 1.01 | 3.29 | 40.76 | 0.15 | 0.02 | 0.10 | 0.15 | 1.11 | 9.00 | 0.02 | 0.11 | 0.00 | 57.29 | -13.24 | -23.12 |
| | M1 | 0.01 | 0.11 | 0.04 | 0.04 | 5.97 | 0.23 | 3.87 | 0.00 | 0.02 | 10.03 | 4.60 | 0.00 | 0.02 | 0.04 | 0.01 | 24.99 | -19.50 | -78.02 |
| | M3 | 0.00 | 0.02 | 0.01 | 0.01 | 0.00 | 0.01 | 0.22 | 0.01 | 0.00 | 0.25 | 0.24 | 0.01 | 0.53 | 0.00 | 0.01 | 1.30 | -1.24 | -94.82 |
| | M6 | 0.00 | 0.00 | 0.00 | 0.00 | 0.04 | 0.02 | 0.00 | 0.00 | 0.73 | 0.07 | 0.50 | 0.00 | 0.00 | 0.02 | 0.00 | 1.37 | -0.30 | -22.08 |
| | U1 | 0.00 | 0.00 | 0.00 | 0.00 | 0.00 | 0.00 | 0.00 | 0.00 | 0.00 | 1.18 | 0.04 | 0.01 | 0.03 | 0.00 | 0.00 | 1.26 | 13.16 | 1044.05 |
| | U2 | 0.00 | 0.00 | 0.00 | 0.00 | 0.00 | 0.00 | 0.00 | 0.00 | 0.00 | 0.00 | 37.73 | 0.07 | 0.35 | 0.00 | 0.00 | 38.15 | 16.43 | 43.06 |
| | U3 | 0.00 | 0.00 | 0.01 | 0.00 | 0.00 | 0.02 | 0.03 | 0.00 | 0.00 | 0.10 | 0.17 | 0.59 | 0.00 | 0.00 | 0.00 | 0.93 | 9.77 | 1050.27 |
| | U4 | 0.00 | 0.00 | 0.01 | 0.00 | 0.00 | 0.02 | 0.01 | 0.00 | 0.01 | 0.02 | 0.00 | 0.77 | 0.90 | 0.02 | 0.00 | 1.76 | 0.44 | 25.21 |
| | U6 | 0.00 | 0.00 | 0.00 | 0.00 | 0.00 | 0.08 | 0.05 | 0.00 | 0.10 | 0.00 | 1.13 | 0.20 | 0.24 | 2.77 | 0.01 | 4.58 | -1.52 | -33.06 |
| | W | 0.00 | 0.00 | 0.00 | 0.00 | 0.00 | 0.04 | 0.02 | 0.00 | 0.07 | 0.33 | 0.66 | 0.01 | 0.02 | 0.03 | 1.01 | 2.20 | -1.13 | -51.54 |
| | Total | 0.19 | 4.26 | 5.44 | 17.21 | 72.77 | 44.04 | 5.49 | 0.07 | 1.07 | 14.42 | 54.57 | 10.70 | 2.20 | 3.07 | 1.07 | | | |

The land use areas, showing the largest decreases, were Paddy field and Mineral, with decreases of -96.76% and -94.82%, respectively. However, when compared in terms of area, the Grass land (U2) land use pattern showed a significant decrease of -19.50 km$^2$. However, the substantial increases in U1 and U3 land use categories, reaching 1,044.05% and 1,050.27% respectively, are primarily driven by the expansion of tourism in the Koh Samui Island. This growth has catalyzed urban sprawl and infrastructure development, particularly within residential areas, government offices, and commercial tourism zones. Details of the changes in land use proportions between 2024 and 2042 are shown in Table 4. The research results on future land use patterns obtained from the CA-Markov model are shown in Figure 5, and the future land use patterns between 2024 and 2042 in the Samui Island area are shown in Figure 6.

The validation of the CA–Markov simulation was performed by comparing the predicted 2024 map with the observed 2024 map. The results demonstrated an overall accuracy of 81.43% and a Kappa coefficient of 0.742, indicating that the CA–Markov model provides an acceptable and reliable level of simulation performance.

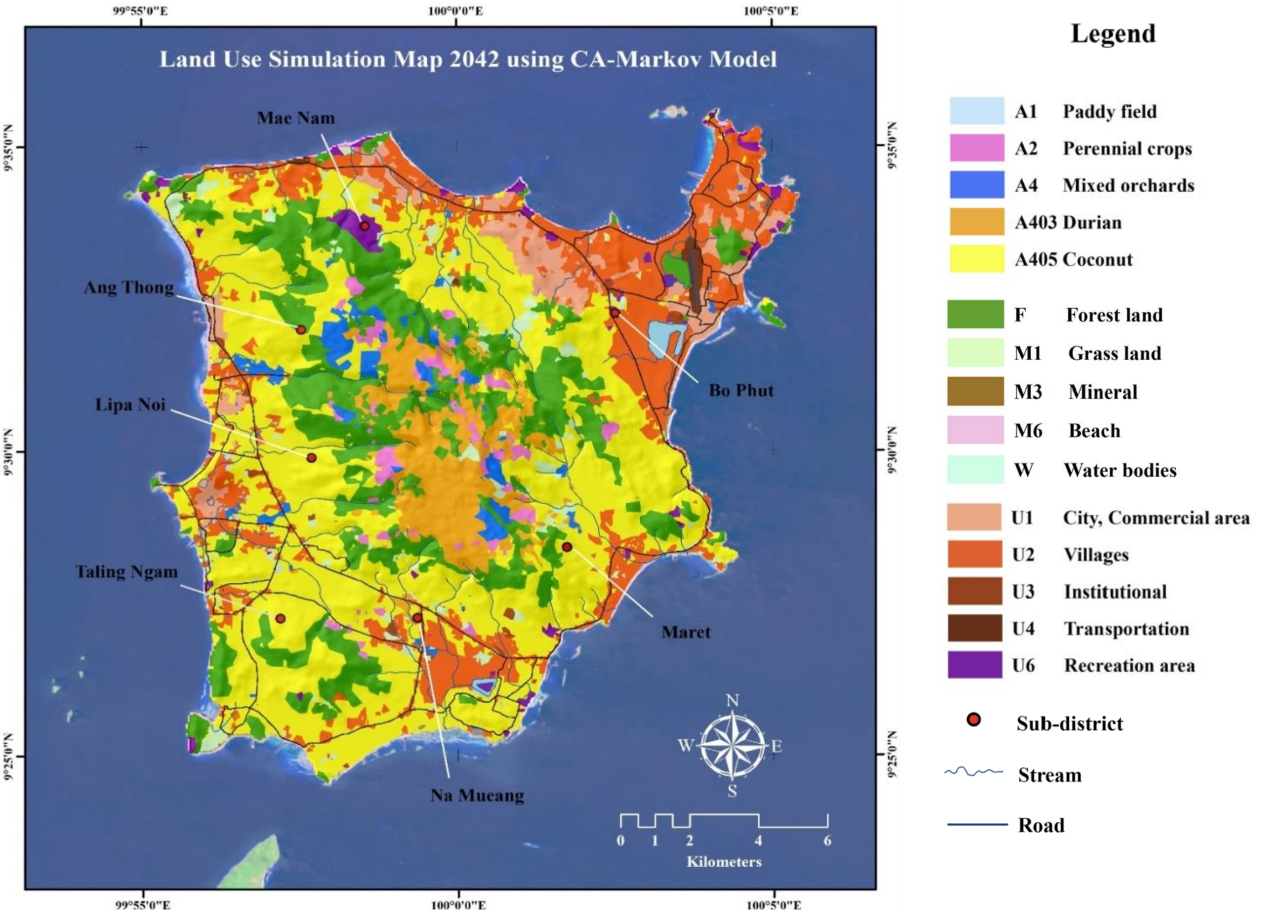


Figure 5. Predicted land use spatial patterns for 2042 generated by CA-Markov simulation (Source: Collected and processed by authors)

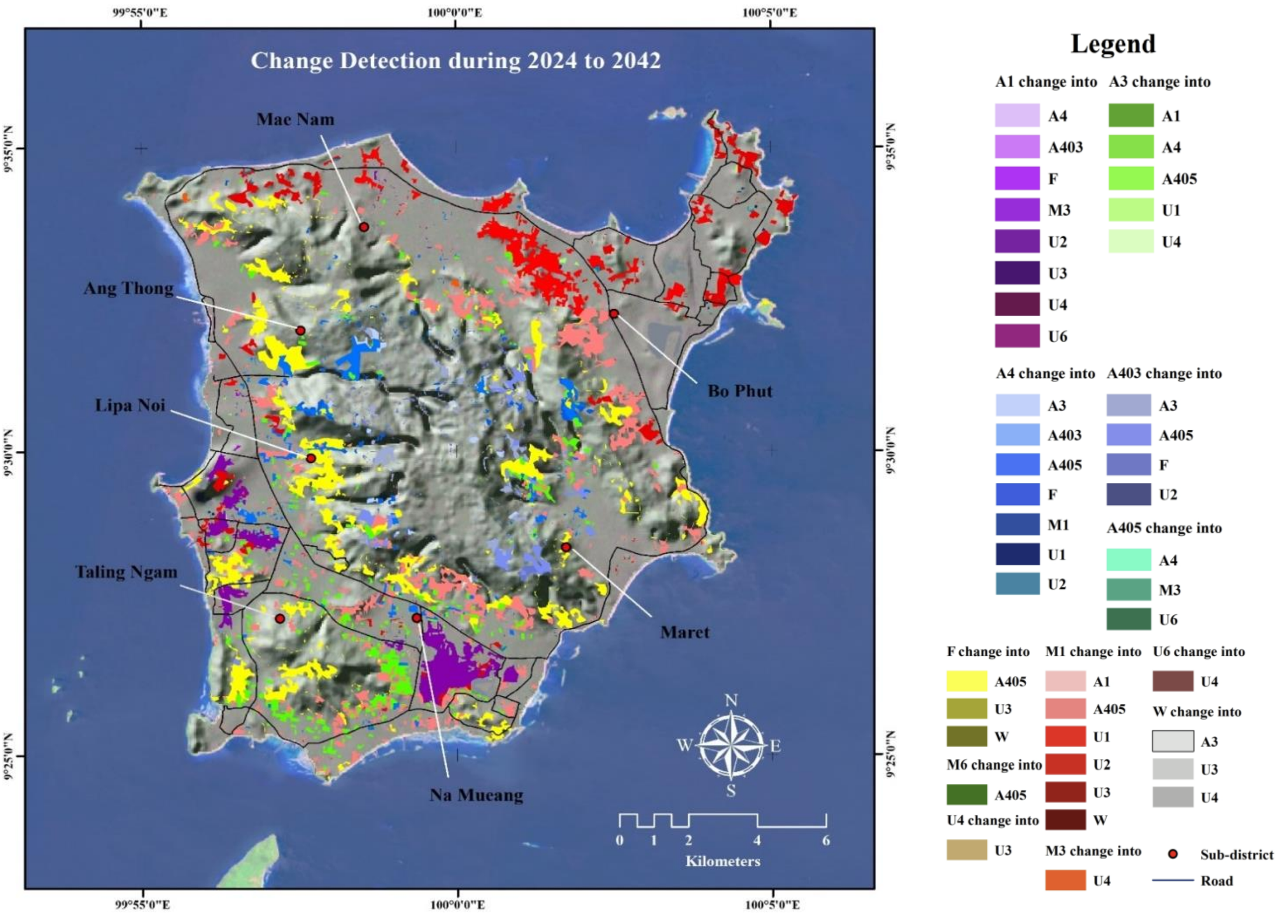


Figure 6. LUC dynamic map during 2024 to 2042 in Samui Island (Source: Collected and processed by authors)

## DISCUSSION

Several research studies have applied the CA-Markov model to simulate future land use patterns. In Thailand, this model has been used to study future LUC in major cities, such as Pattaya (Wiboonwatchara et al., 2024), Nakhon Ratchasima (Kukuntod & Wijitkosum, 2025), and key cities in the Eastern Economic Corridor (EEC) (Waiyasusri et al., 2024), all of which are experiencing significant economic growth. The findings from these studies are consistent with this research, which concludes that cities with strong economic and tourism growth inevitably face challenges related to urban expansion and the expansion of agricultural land. Furthermore, this model has also been applied to various regions. Because analysis of potential impact areas, such as results from CA-Markov models, has helped plan and predict agricultural land use in the Mayurakshi river basin, India (Soren et al., 2024).

In Li, Xinjiang, China, research shows a rapid decrease in forest area (Luo et al., 2025). And in Okara district, Pakistan, future land use predictions from such models show urbanization in arid areas by 2044 (Duan et al., 2025). However, these research findings generally conclude with a similar trend of urban expansion, which differs from this research's findings that, in addition to urbanization in the northeast, south, and west of Samui Island, the central area shows a significant expansion of coconut cultivation.

This research forecasts future land use and creates a Matrix of Land Use Change between the current year and the future. This demonstrates the areas experiencing actual land use changes, something previous research did not analyze using this matrix, thus lacking a clear picture of the impact. Furthermore, land use classifications were not as diverse as in this research. The results highlight the predicted spatial and temporal dynamics of LUC in Samui Island, resulting from urban expansion and the expansion of agricultural land, particularly coconut and durian, which are local cash crops. Overall, this research reveals the potential challenges arising from various types of land use changes.

Therefore, it is crucial to monitor sensitive areas, especially paddy fields, grassland, forest land, orchards, and perennial crops, which are easily transformed into urban areas, villages, or coconut and durian plantations. A particularly concerning area is the central part of Samui Island, which is largely susceptible to conversion into coconut and durian plantations due to its hilly and sloping terrain. If neglected, this could lead to soil erosion and future landslides. This research contributes to a concrete understanding by simulating future land use patterns using a CA-Markov model. The data is presented as a spatial database for planning how to address areas sensitive to change. This model is beneficial for sustainable land use planning. Currently, Samui Island needs to adapt to become a sustainable, ecotourism destination. The results of this model will be useful for spatial development planning in coastal tourist cities, focusing on development that minimizes disruption to nature and promotes more environmentally friendly activities.

## CONCLUSION

This research applied the CA-Markov model to predict future land use change (LUC) changes over the next 18 years (up to 2042) to support effective spatial planning in coastal tourist cities, using Samui Island as a case study. The predictive model reveals a substantial expansion of urban areas by 2042, with City, Town, Commercial (U1) and Institutional (U3) areas projected to surge dramatically by 1,044.05% and 1,050.27%, respectively.

This urban expansion is heavily concentrated in the northeastern region and progressively spreads along the northern and eastern corridors, driven primarily by intense commercial and tourism-related activities. Consequently, this rapid urbanization induces significant land use pressure on surrounding areas; to compensate for lost agricultural lands, coconut plantations are projected to encroach into forest borders, particularly along the foothill regions across the island. These spatial projections reflect current planning vulnerabilities, such as unmanaged urban density, deteriorating and narrow road infrastructure, and severe traffic congestion—most notably in Bo Phut Subdistrict.

To mitigate these unsustainable trends, urgent land use regulation, updated spatial zoning, and comprehensive infrastructure development must be enforced alongside strict legal compliance. Future research should further enhance model precision by incorporating additional socioeconomic variables, infrastructure constraints, and policy interventions. Ultimately, this study provides critical baseline spatial data to guide sustainable tourism development, directly aligning with Sustainable Development Goals (SDG 8: Decent Work and Economic Growth, SDG 11: Sustainable Cities and Communities, and SDG 15: Life on Land) for Samui Island.

**Author Contributions:** Conceptualization, N.U. and K.W.; methodology, N.U. and K.W.; software, N.U., K.W., and D.S.; validation N.U., K.W., and D.S.; formal analysis, N.U., K.W., D.S., T.K.; investigation, N.U., K.W., and D.S.; data curation, N.U. and K.W.; writing - original draft preparation, N.U., K.W., and D.S.; writing - review and editing, N.U., K.W., and D.S.; visualization, K.W.; supervision, K.W.; project administration, N.U. and K.W. All authors have read and agreed to the published version of the manuscript.

**Funding:** Research Grant Funded by the Revenue Budget of the Faculty of Humanities and Social Sciences Mahasarakham University for Fiscal Year 2026.

**Institutional Review Board Statement:** Not applicable.

**Informed Consent Statement:** Not applicable.

**Data Availability Statement:** The data presented in this study may be obtained on request from the corresponding author.

**Acknowledgements:** Acknowledgments to the U.S. Geological Survey (Earth Explorer Homepage: https://earthexplorer.usgs.gov/)**.** And gratefully acknowledge for Suan Sunandha Rajabhat University Research Grant.

**Conflicts of Interest:** The authors declare no conflict of interest.

**Use of Generative AI:** During the preparation of this manuscript, the authors utilized Gemini 1.5 Flash, developed by Google, as an assistive tool to refine sentence structure, enhance academic clarity, and organize selected text sections while strictly preserving the original content and meaning. The tool was neither employed to generate or fabricate research data, perform autonomous statistical analyses, nor make final scientific interpretations. All figures and tables were originally created by the authors. Following the use of this tool, the authors critically reviewed, verified, and revised all AI-assisted outputs, taking full responsibility for the accuracy, integrity, and final content of the published work.

**Glossary:** Geo-IT – Geo-information Technology; LUC – Land use changes; SDGs – Sustainable Development Goals; KHAT – Kappa coefficient; OA – overall accuracy; A1 – Paddy field; A3 – Perennial crops; A4 – Perennial crops; A403 – Durian; A405 – Coconut; F – Forest land; M1 – Grass land; M3 – Mineral; Beach; U1 – City, Town, Commercial; U2 – Villages; U3 – Institutional land; U4 – Transportation; U6 – Recreation area; W – Water bodies

## REFERENCES


Adhikari, S., & Southworth, J. (2012). Simulating forest cover changes of Bannerghatta National Park based on a CA-Markov model: a remote sensing approach. *Remote Sensing, 4*(10), 3215-3243. https://doi.org/10.3390/rs4103215

Appelt, J. L., Garcia Rojas, D. C., Verburg, P. H., & van Vliet, J. (2022). Socioeconomic outcomes of agricultural land use change in Southeast Asia. *Ambio, 51*(5), 1094-1109. https://doi.org/10.1007/s13280-022-01712-4

Aldiansyah, S., Ati, A., & Saudi, F. (2025). Landslide Susceptibility Mapping via Dempster-Shafer, Statistical Index, and Certainty Factor Models in GIS and Their Comparison at Pidie Recency in Aceh, Indonesia. *Applied Environmental Research, 47*(4), 034.

Avci, C., Budak, M., Yağmur, N., & Balçık, F. (2023). Comparison between random forest and support vector machine algorithms for LULC classification. *International Journal of Engineering and Geosciences, 8*(1), 1-10. https://doi.org/10.26833/ijeg.987605

Bai, Y., Hu, L., Wu, B., Qiao, S., Fan, D., Liu, S., Kornkanitnan, N., Khokiattiwong, S., & Shi, X. (2021). Impact of source variability and hydrodynamic forces on the distribution, transport, and burial of sedimentary organic matter in a tropical coastal margin: The Gulf of Thailand. *Journal of Geophysical Research: Biogeosciences, 126*(9), e2021JG006434. https://doi.org/10.1029/2021JG006434

Bikis, A., Engdaw, M., Pandey, D., & Pandey, B. K. (2025). The impact of urbanization on land use land cover change using geographic information system and remote sensing: a case of Mizan Aman City Southwest Ethiopia. *Scientific Reports, 15*(1), 12014. https://doi.org/10.1038/s41598-025-94189-6

Birthal, P. S., Hazrana, J., Negi, D. S., & Bhan, S. C. (2021). Climate change and land-use in Indian agriculture. *Land Use Policy, 109*, 105652. https://doi.org/10.1016/j.landusepol.2021.105652

Butt, A., Shabbir, R., Ahmad, S. S., & Aziz, N. (2015). Land use change mapping and analysis using Remote Sensing and GIS: A case study of Simly watershed, Islamabad, Pakistan. *The Egyptian journal of remote sensing and space science, 18*(2), 251-259. https://doi.org/10.1016/j.ejrs.2015.07.003

Cao, M., Tian, Y., Wu, K., Chen, M., Chen, Y., Hu, X., Sun, Z., Zuo, L., Lin, J., Luo, L., Zhu, R., Xu, Z., Bandrova, T., Konecny, M., Yuan, W., Guo, H., Lin, H., & Lü, G. (2023). Future land-use change and its impact on terrestrial ecosystem carbon pool evolution along the Silk Road under SDG scenarios. *Science Bulletin, 68*(7), 740-749. https://doi.org/10.1016/j.scib.2023.03.012

Chaaban, F., El Khattabi, J., & Darwishe, H. (2022). Accuracy assessment of ESA WorldCover 2020 and ESRI 2020 land cover maps for a Region in Syria. *Journal of Geovisualization and Spatial Analysis, 6*(2), 31. https://doi.org/10.1007/s41651-022-00126-w

Chatterjee, U., & Majumdar, S. (2022). Impact of land use change and rapid urbanization on urban heat island in Kolkata city: a remote sensing based perspective. *Journal of Urban Management, 11*(1), 59–71. https://doi.org/10.1016/j.jum.2021.09.002

Dieno, W. U., & Pathan, S. A. (2025). Flood Susceptibility Mapping and 3D Flood Simulation in the Jia Bharali River Basin, Sonitpur District, India, using the Analytical Hierarchy Process (AHP). *Remote Sensing in Earth Systems Sciences, 8*, 881-911. https://doi.org/10.1007/s41976-025-00226-3

Du, Y., Teillet, P. M., & Cihlar, J. (2002). Radiometric normalization of multitemporal high-resolution satellite images with quality control for land cover change detection. *Remote sensing of Environment, 82*(1), 123-134. https://doi.org/10.1016/S0034-4257(02)00029-9

Duan, X., Haseeb, M., Tahir, Z., Mahmood, S. A., & Tariq, A. (2025). Analyzing and predicting land use and land cover dynamics using multispectral high-resolution imagery and hybrid CA-Markov modeling. *Land Use Policy, 157*, 107655. https://doi.org/10.1016/j.landusepol.2025.107655

Enoh, M. A., Njoku, R. E., & Okeke, U. C. (2023). Modeling and mapping the spatial–temporal changes in land use and land cover in Lagos: A dynamics for building a sustainable urban city. *Advances in Space Research, 72*(3), 694-710. https://doi.org/10.1016/j.asr.2022.07.042

Estoque, R. C., Ooba, M., Togawa, T., Hijioka, Y., & Murayama, Y. (2021). Monitoring global land-use efficiency in the context of the UN 2030 Agenda for Sustainable Development. *Habitat International, 115*, 102403. https://doi.org/10.1016/j.habitatint.2021.102403

Ferdos, J., Ali, K. M. B., Choyon, M. S. H., & Ismail, H. B. (2026). Tourism development and sustainability: Socioeconomic and environmental impacts in Cox's Bazar, Bangladesh. *Geojournal of Tourism and Geosites, 64*(1), 145–155. https://doi.org/10.30892/gtg.64112-1662

Foody, G. M. (2020). Explaining the unsuitability of the kappa coefficient in the assessment and comparison of the accuracy of thematic maps obtained by image classification. *Remote sensing of environment, 239*, 111630. https://doi.org/10.1016/j.rse.2019.111630

Guan, D., Li, H., Inohae, T., Su, W., Nagaie, T., & Hokao, K. (2011). Modeling urban land use change by the integration of cellular automaton and Markov model. *Ecological modelling, 222*(20-22), 3761-3772. https://doi.org/10.1016/j.ecolmodel.2011.09.009

Han, H., Zeeshan, Z., Assam, M., Khan, F. U., Khan, W., Asif, M., Bhatti, U. A., Hasnain, A., Awwad, E. M., & Sarhan, N. (2024). Deep learning techniques for enhanced mangrove land use and land change from remote sensing imagery: A blue carbon perspective. *Big Data Research*, 100478. https://doi.org/10.1016/j.bdr.2024.100478

Hantson, S., & Chuvieco, E. (2011). Evaluation of different topographic correction methods for Landsat imagery. *International Journal of Applied Earth Observation and Geoinformation, 13*(5), 691-700. https://doi.org/10.1016/j.jag.2011.05.001

Herano, D. Y., Woldesenbet, T. A., & Gebrekristos, S. T. (2025). Quantifying the land use land cover change and its effect on sediment yield in upper watersheds of Bilate River, Ethiopia. *Hydrology Research, 56*(8), 603-635. https://doi.org/10.2166/nh.2025.136

Iabsap, T., & Phucharoen, C. (2025). Comparing travellers' experiences in Phuket Island and Samui Island: A sentiment analysis of TripAdvisor. *Kasetsart Journal of Social Sciences, 46*(2), 460205-460205. https://doi.org/10.34044/j.kjss.2025.46.2.05

Ibarra-Núñez, E., & Ortega-Rubio, A. (2025). Tourism spatial planning interaction: local scale analysis in Balandra Protected Natural Area, Mexico. *Journal of Environmental Planning and Management*, *69*(6), 1662-1679. https://doi.org/10.1080/09640568.2025.2451872

Jafari, M., Majedi, H., Monavari, S. M., Alesheikh, A. A., & Zarkesh, M. K. (2016). Dynamic simulation of urban expansion through a CA-Markov model Case study: Hyrcanian region, Gilan, Iran. *European Journal of Remote Sensing*, *49*(1), 513-529. https://doi.org/10.5721/EuJRS20164927

Kamaraj, M., & Rangarajan, S. (2022). Predicting the future land use and land cover changes for Bhavani basin, Tamil Nadu, India, using QGIS MOLUSCE plugin. *Environmental Science and Pollution Research*, *29*(57), 86337-86348. https://doi.org/10.1007/s11356-021-17904-6

Kelly-Fair, M., Gopal, S., Koch, M., Pancasakti Kusumaningrum, H., Helmi, M., Khairunnisa, D., & Kaufman, L. (2022). Analysis of land use and land cover changes through the lens of SDGs in Semarang, Indonesia. *Sustainability*, *14*(13), 7592. https://doi.org/10.3390/su14137592

Khianthongkul, K., & Bunyavejchewin, P. (2024). Airport development projects in Thailand: a case study of Betong International Airport. *Cogent Social Sciences*, *10*(1), 2367260. https://doi.org/10.1080/23311886.2024.2367260

Kiriwongwattana, K., & Waiyasusri, K. (2024). Spatial Evolution of Smart Cities for Sustainable Tourism: A Case Study of Phuket Province, Thailand. *Geojournal of Tourism and Geosites*, *55*(3), 1312–1320. https://doi.org/10.30892/gtg.55331-1303

Krishna, V. V., & Gopinath, G. (2022). Agile Test Automation for Web Application using Testng Framework with Random Integration Algorithm in Machine Learning to Predict Accuracy and Response Time on Automated Test Results. *Journal of Theoretical and Applied Information Technology*, *100*(16), 4909-4917.

Kukuntod, N., & Wijitkosum, S. (2025). Escalating Drought Vulnerability Driven by Land Use Change: Insights from a GIS-Based CA-Markov and Multi-Criteria Assessment of Future Scenarios in the Lam Ta Kong Watershed. *Earth Systems and Environment*. *10*, 4637-4654. https://doi.org/10.1007/s41748-025-00882-x

Le, T. D. H., & Vinh, L. T. (2025). Applying Radom Forest and Support Vector Machine for Land-use Classification in Phu Giao District Vietnam. *Applied Environmental Research*, *47*(2).

Liu, Y., Xue, Y., Zhao, H., Yao, H., Zhan, X., Suk, S., Wang, L., & Yuan, Y. (2025). Coupling coordination and spatiotemporal dynamic evolution between culture and tourism industry in Japan. *Scientific Reports*, *15*(1), 7777. https://doi.org/10.1038/s41598-025-88515-1

Luo, J., Hu, Y., Chen, Y., Zhou, W., Zhang, H., & Liang, T. (2025). Spatiotemporal evolution of land use in Ili, Xinjiang, China: a comparative evaluation of PLUS and Logistic-CA-Markov models. *Geocarto International*, *40*(1), 2570049. https://doi.org/10.1080/10106049.2025.2570049

Marzuki, A., Bagheri, M., Ahmad, A., Masron, T., & Akhir, M. F. (2024). Examining transformations in coastal city landscapes: spatial patch analysis of sustainable tourism—a case study in Pahang, Malaysia. *Landscape and Ecological Engineering*, *20*(4), 513-545. https://doi.org/10.1007/s11355-024-00613-w

Moustakas, A., Zemah-Shamir, S., Tase, M., Zotos, S., Demirel, N., Zoumides, C., Christoforidi, I., Dindaroglu, T., Albayrak, T., Ayhan, C. K., Fois, M., Manolaki, P., Sandor, A. D., Sieber, I., Stamatiadou, V., Tzirkalli, E., Vogiatzakis, I. N., Zemah-Shamir, Z., & Zittis, G. (2025). Climate land use and other drivers' impacts on island ecosystem services: A global review. *Science of the Total Environment*, *973*, 179147. https://doi.org/10.1016/j.scitotenv.2025.179147

Mustafa, H., Omar, B., & Mukhiar, S. N. S. (2019). Measuring destination competitiveness: an importance-performance analysis (IPA) of six top island destinations in South East Asia. *Asia Pacific Journal of Tourism Research*, *25*(3), 223–243. https://doi.org/10.1080/10941665.2019.1687534

Mustelier, D., & Henríquez, C. (2024). Modeling land use change of mid-sized cities in the process of metropolization. Case study La Serena-Coquimbo conurbation, Chile. *Geography, Environment, Sustainability*, *17*(2), 106-118. https://doi.org/10.24057/2071-9388-2024-2984

Nazaruddin, D. A. (2020). Granite landforms of Samui Island (southern Thailand) from geoheritage, geoconservationand geotourism perspectives. *International Journal of Geoheritage and Parks*, *8*, 75–86. https://doi.org/10.1016/j.ijgeop.2020.05.003

Oktavia, D., Pratiwi, S. D., Kamaludin, N. N., Widiawaty, M. A., & Dede, M. (2024). Dynamics of land use and land cover in the Belitung Island, Indonesia. *Heliyon*, *10*(12), e33291. https://doi.org/10.1016/j.heliyon.2024.e33291

Petroni, M. L., Siqueira-Gay, J., & Gallardo, A. L. C. F. (2022). Understanding land use change impacts on ecosystem services within urban protected areas. *Landscape and Urban Planning*, *223*, 104404. https://doi.org/10.1016/j.landurbplan.2022.104404

Phinzi, K., Ngetar, N. S., Pham, Q. B., Chakilu, G. G., & Szabó, S. (2023). Understanding the role of training sample size in the uncertainty of high-resolution LULC mapping using random forest. *Earth Science Informatics*, *16*(4), 3667-3677. https://doi.org/10.1007/s12145-023-01117-1

Pongponrat, K. (2022). Stakeholder engagement process in water saving initiatives for sustainable tourist destination in Samui Island, Thailand. *Pertanika Journal of Social Sciences and Humanities*, *30*(3), 1341-1363.

Pongsakornrungsilp, P., & Pongsakornrungsilp, S. (2023). Mindful tourism: nothing left behind–creating a circular economy society for the tourism industry of Krabi, Thailand. *Journal of Tourism Futures*, *9*(3), 366-380. https://doi.org/10.1108/JTF-01-2021-0001

Puyravaud, J. P. (2003). Standardizing the calculation of the annual rate of deforestation. *Forest ecology and management*, *177*(1-3), 593-596. https://doi.org/10.1016/S0378-1127(02)00335-3

Qiu, H., Hu, B., & Zhang, Z. (2021). Impacts of land use change on ecosystem service value based on SDGs report--Taking Guangxi as an example. *Ecological Indicators*, *133*, 108366. https://doi.org/10.1016/j.ecolind.2021.108366

Quintas-Soriano, C., Buerkert, A., & Plieninger, T. (2022). Effects of land abandonment on nature contributions to people and good quality of life components in the Mediterranean region: A review. *Land use policy*, *116*, 106053. https://doi.org/10.1016/j.landusepol.2022.106053

Rimba, A. B., Mohan, G., Chapagain, S. K., Arumansawang, A., Payus, C., Fukushi, K., Husnayaen, Osawa, T., & Avtar, R. (2021). Impact of population growth and land use and land cover (LULC) changes on water quality in tourism-dependent economies using a geographically weighted regression approach. *Environmental Science and Pollution Research*, *28*(20), 25920-25938. https://doi.org/10.1007/s11356-020-12285-8

Rodriguez-Galiano, V. F., Ghimire, B., Rogan, J., Chica-Olmo, M., & Rigol-Sanchez, J. P. (2012). An assessment of the effectiveness of a random forest classifier for land-cover classification. *ISPRS Journal of Photogrammetry and Remote sensing*, *67*, 93-104. https://doi.org/10.1016/j.isprsjprs.2011.11.002

Sales, V. F., Zanotta, D. C., Marques Jr, A., Racolte, G., Muller, M., Cazarin, C. L., Ibanez, D., Gonzaga Jr, L., & Veronez, M. R. (2023). An adaptive spectral index for carbonate rocks using OLI Landsat-8 imagery. *Geocarto International*, *38*(1), 2179671. https://doi.org/10.1080/10106049.2023.2179671

Sarvestani, G. S., Edalat, M., Shirzadifar, A., & Pourghasemi, H. R. (2025). Early Season Dominant Weed Mapping in Maize Field Using Unmanned Aerial Vehicle (UAV) Imagery: Towards Developing Prescription Map. *Smart Agricultural Technology*, *11*, 100956. https://doi.org/10.1016/j.atech.2025.100956

Song, W., Cao, S., Du, M., & Lu, L. (2023). Distinctive roles of land-use efficiency in sustainable development goals: An investigation of trade-offs and synergies in China. *Journal of Cleaner Production*, *382*, 134889.

Soren, D. D. L., Roy, K. C., & Biswas, B. (2025). Land/use land/cover dynamics and future scenario of Mayurakshi river basin by random forest and CA–Markov model. *International Journal of Environmental Science and Technology, 22*(9), 7815-7828. https://doi.org/10.1007/s13762-024-06006-8

Suhud, U., Allan, M., & Hoo, W. C. (2025). Destination sustainability of Ijen Geopark as perceived by tourists: how far its impact on visit intention? *Geojournal of Tourism and Geosites, 58*(1), 146–160. https://doi.org/10.30892/gtg.58113-1398

Thien, B. B., Phuong, V. T., & Ioshpa, A. R. (2025). Assessing the environmental destruction in forest cover using landscape metrics and spatial analysis in Quang Nam province, Vietnam. *Environmental Earth Sciences, 84*(13), 360. https://doi.org/10.1007/s12665-025-12377-z

Tonolli, A., Pisciotta, A., Scalenghe, R., & Gristina, L. (2024). From grapes to getaways: Unraveling the residential tourism impact on land use change and soil erosion processes in Menfi district. *Land Use Policy, 137*, 107013. https://doi.org/10.1016/j.landusepol.2023.107013

Tsumita, N., Piyapong, S., Kaewkluengklom, R., Jaensirisak, S., & Fukuda, A. (2025). Flood susceptibility mapping of urban flood risk: comparing autoencoder multilayer perceptron and logistic regression models in Ubon Ratchathani, Thailand. *Natural Hazards, 121*(15), 17833-17867. https://doi.org/10.1007/s11069-025-07494-8

Ubonsri, B., & Daungthima, W. (2024). Community Development Guidelines with a Focus on Sustainable Tourism: A Case Study of the Hua Takae Old Market Community. *Journal of Architectural/Planning Research and Studies (JARS), 21*(1), 153-166. https://doi.org/10.56261/jars.v21.255983

United States Geological Survey (2025). *EarthExplorer*. (accessed October 23, 2025). https://earthexplorer.usgs.gov/

Utama, W., Indriani, R. F., Hermana, M., Anjasmara, I. M., Garini, S. A., & Putra, D. P. N. (2024). Towards improving sustainable water management in geothermal fields: SVM and RF land use monitoring. *Journal of Human, Earth, and Future, 5*(2), 216-242. http://dx.doi.org/10.28991/HEF-2024-05-02-06

Vu, J. C., & Turner, L. W. (2006). Regional data forecasting accuracy: The case of Thailand. *Journal of Travel Research, 45*(2), 186-193. https://doi.org/10.1177/0047287506291600

Waiyasusri, K., Vangpaisal, R., & Chotpantarat, S. (2024). Climate and land use change impacts on groundwater recharge in Prachinburi–Sakaeo groundwater basin by integrating the CA–Markov model with the WetSpass Model. *Earth Systems and Environment, 8*(4), 1179-1206. https://doi.org/10.1007/s41748-024-00436-7

Wang, T., He, J., & Ning, Z. (2023). Observations on the development of townships around mega-tourist attraction caused by land use change—the case of Zhangjiajie, China. *Journal of Asian Architecture and Building Engineering*, *22*(5), 3006-3027. https://doi.org/10.1080/13467581.2023.2167494

Waridin, & Astawa, I. P. (2021). Shifting Of Land Use in Sustainable Tourism: A Local Cultural Approach in Indonesia. *GeoJournal of Tourism and Geosites, 35*(2), 270–274. https://doi.org/10.30892/gtg.35201-647

Wayesa, G., Kidane, M., Tolessa, T., & Mammo, S. (2025). Impacts of land Use/land cover dynamics on ecosystem services in Jimma Rare District, Western Ethiopia. *Sustainable Environment, 11*(1), 2436231. https://doi.org/10.1080/27658511.2024.2436231

Wiboonwatchara, B., Shu, H., & Soytong, P. (2024). Monitoring the land use/land cover changes and simulation by using the CA-Markov model-a case study in Bang Lamung district, Pattaya city, Chon Buri province, Thailand. *International Journal of Agricultural Technology*, *20*(1), 411-426.

Xu, C., Hu, X., Liu, Z., Wang, X., Tian, J., & Zhao, Z. (2023). Predicting the evolution trend of water and land resource carrying capacity based on CA–Markov Model in an Arid Region of Northwest China. *Sustainability, 15*(2), 1269. https://doi.org/10.3390/su15021269

Yang, M., Luo, J., Zhu, L., & Lu, P. (2024). Impact of Land Use Change on the Spatiotemporal Evolution of Ecosystem Services in Tropical Islands: A Case Study of Hainan Island, China. *Land, 13*(8), 1244. https://doi.org/10.3390/land13081244

Yeemin, T., Sutthacheep, M., Pengsakun, S., Klinthong, W., Chamchoy, C., & Suebpala, W. (2024). Quantifying blue carbon stocks in interconnected seagrass, coral reef, and sandy coastline ecosystems in the Western Gulf of Thailand. *Frontiers in Marine Science, 11*, 1297286. https://doi.org/10.3389/fmars.2024.1297286

Article history: Received: 18.12.2025 Revised: 09.04.2026 Accepted: 05.07.2026 Available online: 06.08.2026